Boron and nitrogen impurities in SiC nanowires

I. S. Santos de Oliveira and R. H. Miwa
Instituto de Física, Universidade Federal de Uberlândia, C. P. 593, 38400-902, Uberlândia, MG, Brazil
(Received 15 October 2008; published 25 February 2009)

We have performed a theoretical *ab initio* study of the B and N impurities in hydrogen-passivated SiC nanowires (NWs). The calculations were performed within the density-functional theory, and using norm-conserving pseudopotentials to describe the electron-ion interactions. We have considered SiC nanowires growth along the [100] and [111] directions. For B-doped SiC NWs, our results indicate that the atomic relaxations around the impurity site play an important role to the energetic preference of B atoms occupying the Si sites (B_{Si}) at the NW surface. The formation of B_C becomes energetically more favorable than B_{Si} only at the Si-rich condition. On the other hand, even at the Si-poor condition, the formation of N_{Si} is not expected to occur, N_C being the energetically more favorable configuration. In particular for the C-coated SiC NW growth along the [100] direction and the SiC NW growth along the [111] direction, the N_C atoms are energetically more stable at the inner sites of the NWs. Thus, indicating that in those systems the N_C atoms do not segregate toward the NW surface.

DOI: 10.1103/PhysRevB.79.085427 PACS number(s): 71.15.Mb, 71.15.Nc, 71.20.Mq

I. INTRODUCTION

Doping processes of nanostructures such as nanotubes, nanowires, and nanocrystals may face a quite different scenario from that obtained in the bulk phase. For instance, several nanocrystals exhibit a low incorporation rate of impurities when compared with their bulk counterpart. In this case, the impurity elements are ejected from the inner sites of the nanocrystal, lying at the nanocrystal surface or subsurface sites, i.e., there is a "self-purification" process.[1]

Based upon experimental measurements and supported by *ab initio* theoretical calculations, Erwin *et al.*[1] proposed that the self-purification mechanism of isovalent impurities in II-VI semiconductors nanocrystals is ruled by the binding energy of the impurity elements on the nanocrystal surface. Further theoretical calculations in nanocrystals in CdSe verified that the formation energy of Mn impurity "increases as the size of the nanocrystal decrease."[2–4] In this case, the self-purification is ruled by the reduction in the impurity formation energy in nanocrystals. In Refs. 5 and 6 the authors calculated the formation energy of B and P impurities as a function of the nanocrystal size. They find that below a critical size, the impurity elements exhibit the lowest formation energy lying at the nanocrystal subsurface sites. Similarly in Si[110] (Refs. 7 and 8) and Ge[110] (Ref. 9) nanowires (NWs), the segregation of B and P impurity atoms, toward the nanowire surface, is an exothermic process. In this paper, we investigate if the self-purification also takes place in silicon carbide nanowires (SiC NWs).

Silicon carbide has been considered as a promising material to buildup new (nano)electronic devices, high-power electronic devices, biocompatible materials, and most recently as a candidate for hydrogen storage devices.[10,11] In the bulk phase, SiC presents different polytypes depending how the Si-C double layers are piled up along the growth direction. Meanwhile, new nanostructures based on SiC have been successfully synthesized, viz., wires, tubes, and clusters.[12–15] In parallel to those experimental findings, numerous theoretical studies have been done aiming not only support the experimental results related to the atomic structure, energetic stability, and electronic properties of those nanostructures, but also investigate new properties not yet observed experimentally: for example, the hydrogen interaction with native defects in SiC nanotubes[16,17] and the *p*- and *n*-type doping processes in SiC nanotubes.[18]

Like other bulk semiconductor materials, the electronic properties of SiC can be tailored through suitable doping processes. Boron and nitrogen are the most frequently used dopant elements for *p*- and *n*-type SiC, respectively. There are several studies addressing B and N impurities in SiC: for instance, (i) recent experimental investigations focusing the boron diffusion in 4H-SiC.[19] Meanwhile (few years before) theoretical studies examined the effect of native defects in the B diffusion in SiC.[20,21] (ii) The incorporation processes of N impurities in 4H-SiC was revisited in a recent experimental work.[22] In parallel, clustering processes of N atoms in SiC have been examined by total-energy *ab initio* calculations.[23]

Motivated by the recent experimental control in buildup new nanostructures based on SiC, and the new theoretical results regarding the doping processes of low dimensional systems (nanocrystals, nanotubes, and nanowires), we performed an *ab initio* total-energy study of B- and N-doped SiC NWs. We have considered SiC NWs along the [100] and [111] directions, SiC[100] and SiC[111], respectively. In particular, for the SiC[100] NWs, we examined the Si-coated (Si/SiC[100]) and the C-coated (C/SiC[100]) SiC NWs. The calculations were performed in the framework of the density-functional theory (DFT) as described in the next section, Sec. II. Our results, presented in Sec. III, reveal that B atom occupying the silicon site (B_{Si}) at the NW surface represents the most likely configuration for B-doped SiC NWs. That is, "self-segregation" processes take place in B-doped SiC NWs. Whereas, in N-doped C/SiC[100] and SiC[111] NWs, the nitrogen segregation toward the NW surface is not an exothermic process, thus, indicating that self-segregation processes are not expected in those N-doped SiC NWs. In Sec. IV we present a summary of our conclusions.

II. METHOD OF CALCULATION

The calculations were performed based upon the density-functional theory as implemented in the SIESTA code,[24] within the generalized gradient approximation due to Perdew, Burke, and Ernzerhof.[25] The Kohn-Sham orbitals were described by linear combinations of numerical pseudoatomic orbitals using a split-valence double-zeta basis set including polarization functions. We have considered an energy shift of 0.20 eV (Ref. 24) to determine the radius cutoff of the pseudoatomic orbitals. In addition, we verify the convergence of our total-energy results for lower energy shift, 0.10 eV. The electron-ion interactions were calculated by using norm-conserving pseudopotentials.[26] The SiC NWs were described within the supercell approach. In order to avoid the interaction of a NW with its image (due to the periodic boundary conditions), there is a lateral (radial) separation, vacuum region, of 11 Å between two consecutive NW surfaces, which corresponds to a distance of ~22 Å between NW centers. Along the NW growth direction (longitudinal direction) we have considered axial lengths of 4.41 and 7.62 Å for the SiC[100] and SiC[111] NWs, respectively. The self-consistent total charge density was obtained by using a set of two special **k** points to sample the Brillouin zone. The surface dangling bonds of the NWs were saturated with hydrogen adatoms, while the core region of the NWs kept the 3C-SiC structure. We examine the convergence of our total-energy results with respect to the (i) longitudinal length of our supercell and (ii) number of special k points. In (i), increasing the size the of supercell from 4.41 Å (93 atoms/supercell) to 8.82 Å (186 atoms/supercell), we find that the absolute (relative) values of the formation energies are converged by 80 meV (26 meV) for B impurities in SiC[100] NWs. For N impurities, we find an absolute (relative) formation energy convergence of 160 meV (16 meV). In (ii), increasing the number to special k points ($2 \rightarrow 12$ k points), we find total-energy convergences of 30 and 85 meV for B and N impurities in SiC[100]. Those findings indicate that the present calculation approach provide reliable total-energy results. All the atomic positions (of pristine and doped SiC NWs) were relaxed by using the conjugated gradient scheme, within a force convergence criterion of 20 meV/Å.

The 3C-SiC bulk was described by using a supercell with 64 atoms and eight special k points to the Brillouin-zone sampling. At the equilibrium geometry, we find a lattice constant of 4.41 Å, which is in good agreement with the experimental measurement (4.35 Å). We find an indirect band gap (ΓX) of 1.32 eV, while the experimental value is 2.4 eV. Such underestimation of the width of the energy band gap is expected since the conduction states are not accurately described within the DFT approach.[27] The calculated projected density of states (PDOS) indicate that the most of the electronic states of the valence-band maximum (VBM) and the conduction-band minimum (CBM) come from the C-2p and Si-3p orbitals, respectively.

III. RESULTS AND DISCUSSION

Initially we examined hydrogen-passivated pristine SiC NWs grown along the [100] and [111] directions. We have considered NW diameters (d) of ~12 Å. For the [100] NWs, we may have Si-rich or C-rich NW surfaces, as depicted in Figs. 1(a) and 1(b), respectively. The surfaces of [111] SiC NW are at the Si and C stoichiometric equilibrium condition. That is, we have the same number of hydrogen saturated Si and C surface dangling bonds. Figure 1(c) presents the structural model of the [111] SiC NW.

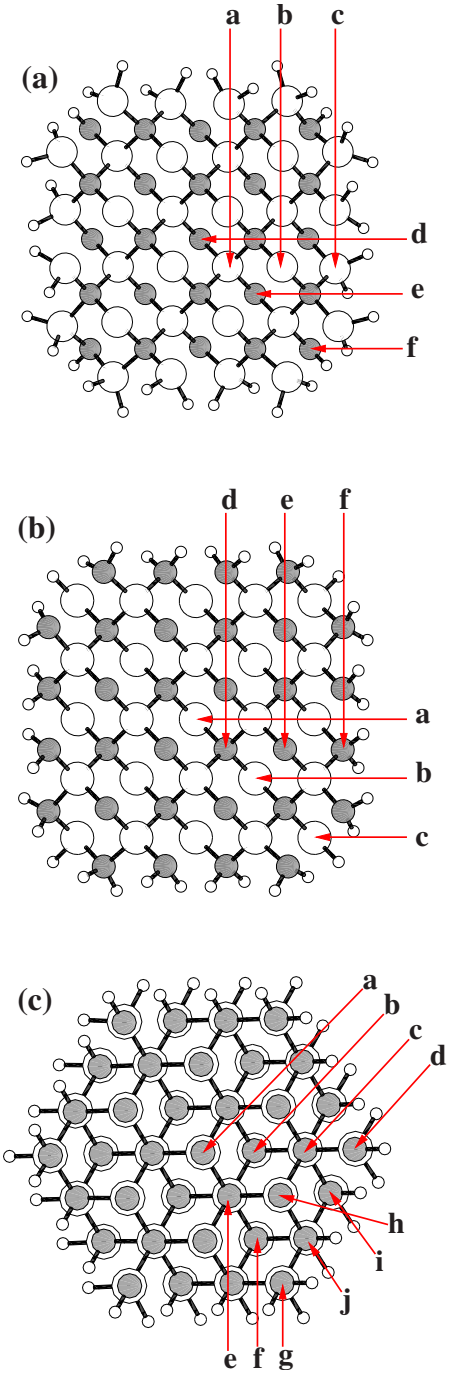

FIG. 1. (Color online) Top view of the structural models of (a) Si-coated [100] SiC NW, (b) C-coated [100] SiC NW, and (c) [111] SiC NW. Filled and empty circles represent the C and Si atoms, respectively. Small-empty circles represents the (surface) hydrogen atoms.

In the core region of SiC NWs we find a bulklike environment that mimics the structural and electronic properties of SiC bulk. Meanwhile, due to the lateral Si or C (surface) terminations, SiC NWs are energetically less stable compared with their bulk counterpart. Indeed, our calculated cohesion energies (E^{coh}) of the SiC NWs are lower compared with the cohesion energy of the 3C SiC bulk phase. E^{coh} can be defined as

$$E^{\mathrm{coh}} = -\left(E^{\mathrm{SiC\ NW}} - \sum_i n_i E_i^{\mathrm{atom}}\right). \quad (1)$$

$E^{\mathrm{SiC\ NW}}$ represents the total energy of the hydrogen-passivated SiC NWs and E^{atom} (n_i) represents the total energy (number) of isolated Si, C, and hydrogen atoms of that composing the NW system. Our calculated cohesion energies, viz., 4.92, 5.33, and 5.31 eV for the Si/SiC[100], C/SiC[100], and SiC[111] NWs, respectively, indicate that the SiC NWs are less stable than the SiC bulk phase by 40% (Si/SiC[100] NW) and 24% (SiC[111] and C/SiC[100] NWs). We find E^{coh}=6.89 eV for the SiC bulk phase. We can infer that the higher cohesion energy of the C/SiC[100] NW compared with Si/SiC[100] is due to the formation of energetically more stable C-H bonds on the C/SiC[100] NW surface, while in Si/SiC[100] most of the hydrogen atoms saturate the Si dangling bonds. Those cohesion energy results are in accordance with previous *ab initio* study performed by Rurali.[28] In general the presence of dangling bonds and atomic reconstructions at the NW surface promotes the formation of surface states within the energy band gap. However, those surface states are (in general) suppressed by saturating the surface dangling bonds with hydrogen atoms, and the increase in the energy band gap due to the one-dimensional confinement is strengthened in hydrogen-passivated NWs. Similar to the SiC bulk phase, the VBM (CBM) is mostly composed by C-2p (Si-3p) orbitals.

For the Si/SiC[100] NW, we find a band gap width of 2.21 eV, and the most of the highest occupied states are localized on the (i) C atoms in the core region of the NW and (ii) along the Si-H bonds on the NW surface. The band gap is 0.2 eV larger in the C/SiC[100] NW, 2.42 eV. Similar to Si/SiC[100], most of the electronic states within an energy interval of 2 eV below the calculated Fermi level (E_F) lie within the core region of the NW; however, in this case the electronic charge-density contribution from the surface C-H bonds is negligible. Those electronic states are resonant within the valence band. For the [111] SiC NW we find an energy band gap of 2.80 eV. The charge-density distribution along the NW cross section suggests that the highest occupied states, within E_F-2 eV, are uniformly distributed along the NW diameter, with small contribution from the NW surface. In Ref. 28 the author obtained band gaps of around 2.2 and 2.5 eV for the Si-rich and C-rich [100] SiC NWs. Finally, the increase in the energy-band gap for smaller NW diameters has been observed for the SiC NWs, namely, 1.32 eV (SiC bulk), 2.21 eV (d=12.8 Å, Si/SiC[100]), 2.42 eV (d=12.6 Å, C/SiC[100]), and 2.80 eV (d=10.8 Å, SiC[111]).

Before we start our investigations of the B- and N-doped SiC NWs, we examined the energetic stability of those defects in the 3C-SiC bulk phase. In particular, for B or N atoms occupying the Si or C sites of the host SiC, the formation energies (Ω_i) can be written as,

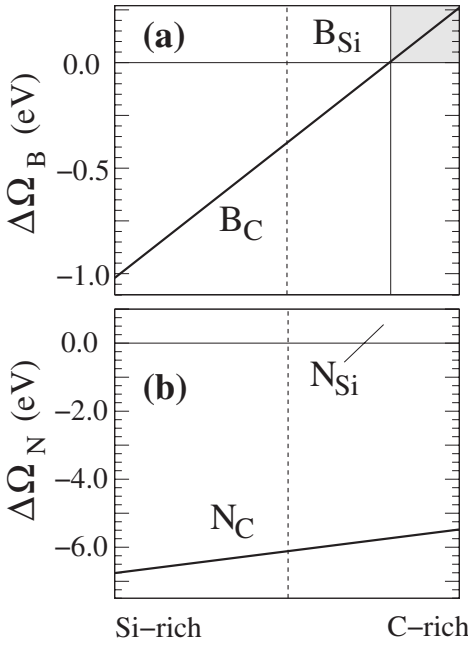

FIG. 2. Relative formation energy ($\Delta\Omega$) of (a) substitutional B and (b) N impurities in the 3C-SiC bulk, as a function of the chemical potential of C atoms (μ_C). At the C-rich (Si-rich) limit we have $\mu_C=\mu_C^{\mathrm{bulk}}$ ($\mu_C=\mu_C^{\mathrm{bulk}}-\Delta H^{\mathrm{3C\text{-}SiC}}$). The shaded region indicate the energy interval where $\Delta\Omega_B>0$.

$$\Omega_i = E_i - E_0 - \mu_i + \mu_j, \quad (2)$$

where E_i (E_0) represents the total energy of the 3C-SiC bulk with substitutional B or N atoms (pristine 3C-SiC system). μ_i and μ_j represent the chemical potentials of the substitutional species (i=B,N) and the host elements (j=Si,C), respectively. Here we did not include the dependence of the formation energy on the Fermi energy since we are considering only neutral defects. For SiC NWs, in Eq. (2), E_i and E_0 represent the total energies doped and pristine NWs, respectively. The upper limit of the chemical potentials are constrained by the total energy of the respective elemental phase. At the C-rich limit we have $\mu_C=\mu_C^{\mathrm{bulk}}$, and at the Si-rich (C-poor) limit we have $\mu_C=\mu_C^{\mathrm{bulk}}-\Delta H^{\mathrm{3C\text{-}SiC}}$. We find $\Delta H^{\mathrm{3C\text{-}SiC}}$=0.64 eV, where $\Delta H^{\mathrm{3C\text{-}SiC}}=\mu_{\mathrm{Si}}^{\mathrm{bulk}}+\mu_C^{\mathrm{bulk}}-\mu_{\mathrm{3C\text{-}SiC}}$. The equilibrium condition imposes that the sum of Si and C chemical potentials is equal to the SiC bulk total energy, namely, $\mu_{\mathrm{Si}}+\mu_C=\mu_{\mathrm{3C\text{-}SiC}}^{\mathrm{bulk}}$.[29] Here, instead of calculating the absolute values of the formation energies, we analyze the relative formation energies for B and N substitutional impurities in SiC. Figures 2(a) and 2(b) summarize our calculated relative formation energies for B ($\Delta\Omega_B=\Omega_{B_C}-\Omega_{B_{Si}}$) and N ($\Delta\Omega_N=\Omega_{N_C}-\Omega_{N_{Si}}$) impurities, respectively. In this case, negative values of $\Delta\Omega_B$ ($\Delta\Omega_N$) indicate that the formation of substitutional boron (nitrogen) atoms occupying the C sites, B_C (N_C), is more likely than boron (nitrogen) atoms occupying the silicon sites, B_{Si} (N_{Si}). At the Si/C stoichiometric condition, indicated by a dashed line in Fig. 2(a), we find

that the formation of B_C is energetically more favorable than B_{Si} by 0.38 eV, i.e., $\Delta\Omega_B=-0.38$ eV. In the same diagram, we observe that B_{Si} becomes more likely than B_C, $\Delta\Omega_B>0$ [indicated by the shaded region in Fig. 2(a)], only at the C-rich limit. The energetic preference of B_C is in accordance with previous total-energy investigations.[30,31] At the equilibrium geometry, B_C-Si and B_{Si}-C bond lengths are 1.96 and 1.76 Å, respectively. Comparing with the sum of the covalent radii, B_C-Si is compressed by 0.02 Å, while B_{Si}-C is stretched by 0.18 Å, thus, suggesting that the local strain induced by B atoms occupying the Si sites is larger compared with the one for B occupying the C sites. Similar energetic preference for the carbon sites has been also observed for N impurities in 3C-SiC [Fig. 2(b)], while the formation of N_{Si} is not expected even at the C-rich limit. That is, we have $\Delta\Omega_N<0$ within the allowed energy interval of the carbon chemical potential. The formation of N_C is more likely than N_{Si} by 5.5 eV (6.75 eV) at the C-rich (Si-rich) condition. In Ref. 23 the authors verified that N_{Si} is not expected to occur, and obtained formation energy differences of around 6 eV, N_C being the energetically more favorable configuration in accordance to the previous experimental findings.[32] Since our result for the equilibrium geometry, formation energy, and electronic properties compare very well with the ones presented in previous *ab initio* calculations, we next start our investigation of B- and N-doped SiC NWs.

A. Boron in SiC NWs

Figures 3(a) and 3(b) present the relative formation energies (at the Si/C stoichiometric condition) of substitutional B atoms in the Si/SiC[100] and C/SiC[100] NWs, respectively. In those diagrams we observe that at the inner sites of SiC NWs, sites *a* and *d* indicated in Fig. 1, the energetic preference for B_C has been kept. However, the formation of B_{Si} becomes more likely near the NW surface, B_{Si} occupying the surface silicon site B^c_{Si}, represents the energetically more favorable configuration for both SiC[100] NWs. For the Si/SiC[100] NW the B^c_{Si} substitutional atom is fourfold coordinated forming two B^c_{Si}-C bonds with the nearest-neighbor C atoms and two B^c_{Si}-H bonds with the surface hydrogen atoms. In the C/SiC[100] NW the B^c_{Si} substitutional atom is also fourfold coordinated, however, forming three B^c_{Si}-C bonds with the nearest-neighbor atoms C atoms and a single B^c_{Si}-H bond. At the equilibrium geometry, for both systems, the B^c_{Si}-C bonds (1.64 Å) are stretched by 0.06 Å compared with the sum of the B and C covalent radii. Meanwhile, at the inner sites of SiC[100] NWs, the B^a_{Si}-C bond lengths are the same as compared with the 3C-SiC bulk phase, 1.76 Å. Those results suggest that the strain effects play an important role for the energetic preference for B substitutional atoms at the surface sites of the SiC[100] NWs.

In the same diagrams, we present the relative formation energy for unrelaxed systems (dashed lines). In this case, the boron-doped NWs are not allowed to relax, keeping the equilibrium geometry of the pristine NWs. For B_{Si} in Si/SiC[100], Fig. 3(a), we observe that the amount of the total-energy reduction upon the atomic relaxation is larger on the

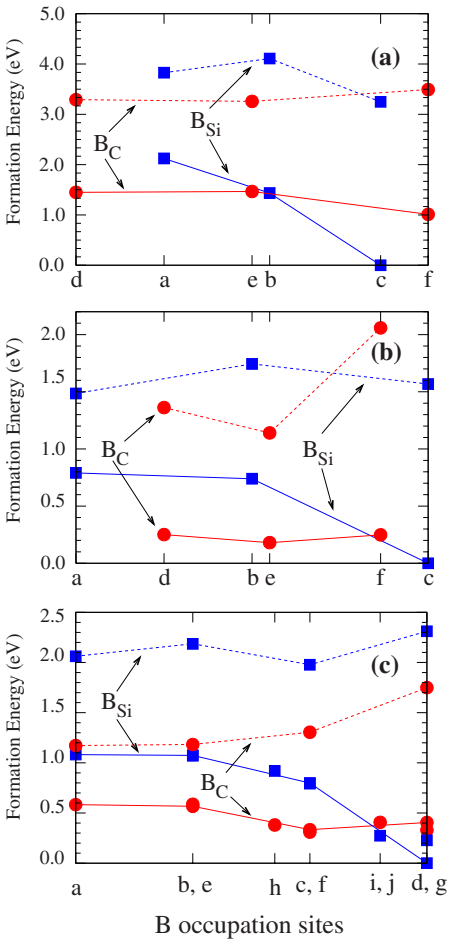

FIG. 3. (Color online) Relative formation energy, at the Si/C stoichiometric condition, of B_C and B_{Si} impurities along the NW diameter of (a) Si/SiC[100], (b) C/SiC[100], and (c) SiC[111] NWs. Solid (dashed) lines indicate the relaxed (unrelaxed) boron-doped NWs. The B occupation sites are indicated in Fig. 1. The zero energy is taken for the energetically more favorable configuration, namely, B_{Si} at the NW surface.

surface site (3.2 eV), compared with the one on the core region of the Si/SiC[100] NW, 1.6 eV. For B_C, the relaxation energy is practically the same along the NW diameter, being slightly larger (by ~0.6 eV) at the surface sites. Similar energetic preference for the surface sites has been predicted for B and P impurities in Ge[110] NWs.[9] In that study the authors pointed out the importance of atomic relaxations near the NW surface in lowering the total energy. In addition, recent theoretical investigations examined the nanocrystals size dependence on the impurity segregation toward the surface. In Refs. 2 and 4 the authors suggested a self-purification mechanism for Mn-doped CdSe nanocrystals, supported by further investigations in P-doped Si nanocrystals.[6] In that case, the authors verified that in Si nanocrystals with diameters smaller than 20 Å the substitutional P impurities segregate to the surface.

It is noticeable that the formation of B_C at the NW surface, site *f* of the C/SiC[100] NW (B^f_C), is energetically less favorable compared with B^c_{Si} [Fig. 3(b)]. This result is somewhat unexpected based upon the statement presented above

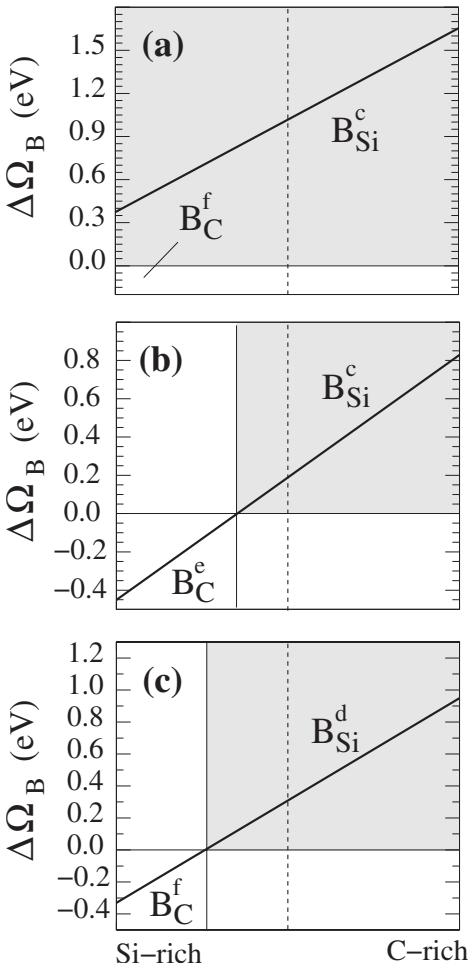

FIG. 4. Relative formation energies of substitutional B_C and B_{Si} ($\Delta\Omega_B$), as a function of the carbon chemical potential (μ_C), in (a) Si/SiC[100], (b) C/SiC[100], and (c) SiC[111] NWs. At the C-rich (Si-rich) limit we have $\mu_C=\mu_C^{bulk}$, ($\mu_C=\mu_C^{bulk}-\Delta H^{3C\text{-}SiC}$). Shaded regions indicate the energy intervals where $\Delta\Omega_B>0$.

since both sites (c and f) are at the NW surface, and thus, allowing more effective atomic relaxations. Moreover, in the 3C-bulk phase B_C is energetically more favorable than B_{Si}. On the other hand, at the NW surface, the binding energies of the C-H bonds are higher than the binding energies of Si-H, promoting the formation of B_{Si}^c rather than B_C^f in C/SiC[100] NWs. Based upon those results, we can infer that the higher binding energy of C-H bonds of C/SiC[100] NWs somewhat avoid the formation of B_C at the NW surface. Figure 4 presents the relative formation energy ($\Delta\Omega_B$) of the most likely configurations of B_{Si} and B_C as a function of the carbon chemical potential. In those diagrams we find that, even at the Si-rich condition, the formation of B_C is not expected on the surface sites of Si/SiC[100] NW since $\Delta\Omega_B$ assume only positive values within the allowed energy range of μ_C [shaded region in Fig. 4(a)]. Whereas, in C/SiC[100] NWs, the formation of B_C in the subsurface site (B_C^e) becomes more likely than B_{Si}^c at the Si-rich condition [$\Delta\Omega_B<0$ region Fig. 4(b)].

Similar to the SiC[100] NWs, the segregation of B impurities toward the NW surface has also been observed in SiC[111] NWs. Figure 3(c) presents the relative formation energy of substitutional B atoms along the NW diameter. We observe that at the inner sites of the SiC[111] NW the energetic preference of B_C has been strengthened as compared with the 3C-SiC bulk phase, that is, in the former (latter) system the formation energy of B_C is lower by 0.50 eV (0.38 eV) compared with B_{Si}. In the same diagram we observe that the energetic preference of B_C has been kept up to the subsurface carbon sites, B_C^c. On the surface site i or j (the hexagonal face of the NW) the formation of substitutional B atom on the Si site is energetically more favorable by 0.15 eV, compared with B_C. However, the energetic preference of B_{Si} becomes more evident at the edge sites of the NW surface, B_{Si}^d. The substitutional B_{Si}^d atom forms three B-C bonds and a single B-H bond. At the equilibrium geometry, similar to B_{Si}^c in the [100] NWs, we obtained B-C bond lengths of 1.65 Å. Atomic relaxations play an important role to the surface segregation of the B impurity in the SiC[111] NW. Dashed lines in Fig. 3(c) indicate that B_C impurities are more stable at the inner sites of the unrelaxed SiC[111] NWs. Comparing the total energies of the relaxed and unrelaxed systems, we observe that the relaxation energies are larger at the NW surface. We find relaxation energies of 1.0 eV (0.5 eV) at the NW core sites, B_{Si}^a (B_C^a), and 2.6 eV (1.8 eV) at the NW surface, B_{Si}^d (B_C^d). The formation energies of substitutional B atoms in the SiC[111] NW indicate that the formation of B_{Si}^d is dominant within the allowed interval of μ_C, shaded region in Fig. 4(c), while B_C^f occurs ($\Delta\Omega_B<0$) only at the C-poor limit.

Finally, we examine the dependence of the energetic stability of substitutional B impurities as a function of the SiC (host) structural phase. We compare the formation energies of B impurity in the SiC NW ($\Omega^{SiC\ NW}$) and in the 3C-SiC bulk ($\Omega^{3C\text{-}SiC}$),

$$\Delta\Omega = \Omega^{SiC\ NW} - \Omega^{3C\text{-}SiC}. \quad (3)$$

Positive values of $\Delta\Omega$ indicate that the B-doping process in SiC is more difficult in SiC NWs, when compared with its counterpart in the 3C-SiC bulk. Indeed this is what we find for B atoms occupying the core sites of the NWs. Our calculated results of $\Delta\Omega$ are summarized in Table I. Here we are assuming that the chemical potentials of Si and C atoms are the same for the SiC bulk and NW systems. For instance, the formation of B_C in the core region of the Si/SiC[100] (C/SiC[100]) NW is energetically less favorable by 0.50 eV (0.11 eV) compared with the formation of the same defect in 3C-SiC bulk. On the other hand, the energetic cost of B_C at the surface and subsurface sites of the NWs is the same as that of B_C in the SiC bulk phase. In contrast, the energetic cost for B_{Si} at the surface and subsurface sites of the NWs are lower compared with the same defect in 3C-SiC. It is important to take into account that we are considering thin SiC NWs. For larger NW diameters it is expected $\Delta\Omega\rightarrow 0$ at the core sites since the electronic confinement and the NW surface effects become negligible at the core sites of the NWs. Thus, comparing the results of $\Delta\Omega$ at the core and surface/subsurface sites, and the formation energy results of the B impurity atom along the NW diameter, we can infer that the proposed self-purification mechanism also takes

TABLE I. Calculated results of $\Delta\Omega$ (in eV) for B impurity in SiC.

	Core	Surface/subsurface
Impurity	$\Delta\Omega^{(\text{site})}$	$\Delta\Omega^{(\text{site})}$
	Si/SiC[100] NW	
B_{Si}	$0.90^{(a)}$	$-1.86^{(c)}$
B_C	$0.50^{(d)}$	$0.05^{(f)}$
	C/SiC[100] NW	
B_{Si}	$0.38^{(a)}$	$-0.61^{(c)}$
B_C	$0.11^{(d)}$	$0.05^{(e)}$
	SiC[111] NW	
B_{Si}	$0.47^{(a)}$	$-0.61^{(d)}$
B_C	$0.24^{(a)}$	$-0.01^{(c)}$

place for B_{Si} and B_C impurities in thin SiC NWs.

Figure 5 presents the PDOS for the energetically more stable configurations of substitutional B atoms in SiC NWs. For B_{Si} occupying the surface sites of the Si/SiC[100] NW we find two spin unpaired electronic levels within the band gap $v1$ (occupied) and $c1$ (empty) lying at around 1 and 1.4 eV above the VBM, respectively [Fig. 5(a)]. In C/SiC[100], Fig. 5(b), $v1$ lies at 0.4 eV above the VBM and the energy split between $v1$ and $c1$ is equal to 0.4 eV. Those $v1$ and $c1$

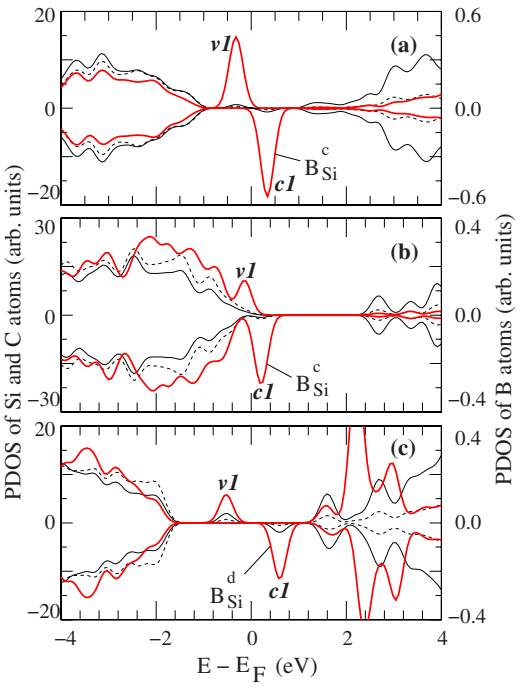

FIG. 5. (Color online) PDOS of (a) B_{Si}-doped Si/SiC[100], (b) C/SiC[100], and (c) SiC[111] NWs. Solid thick (red) lines represent the PDOS of B atoms, and the solid (dashed) thin lines represent the PDOS of Si (c) atoms. We have considered a Gaussian (broadening) width of 0.2 eV, and the positive (negative) values of PDOS correspond to spin-up (spin-down) electronic densities.

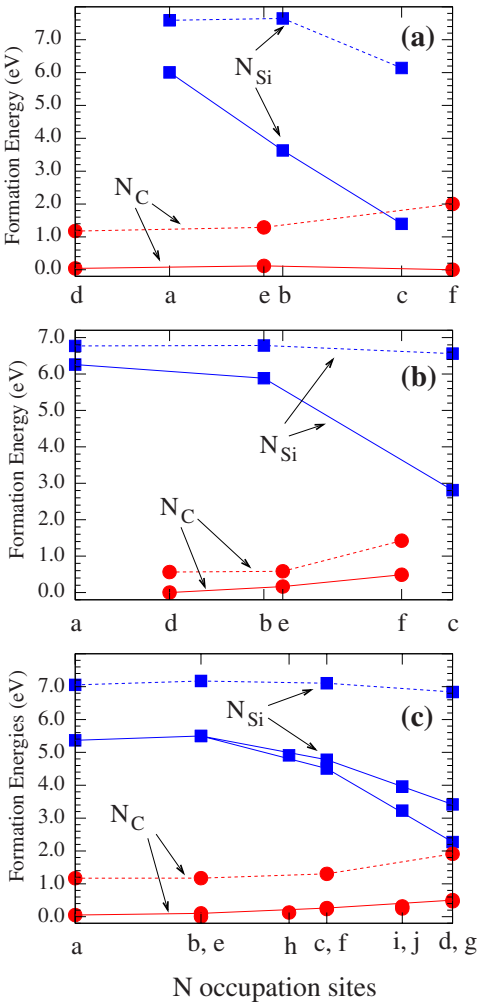

FIG. 6. (Color online) Relative formation energy, at the Si/C stoichiometric condition, of N_C and N_{Si} impurities along the NW diameter of (a) Si/SiC[100], (b) C/SiC[100], and (c) SiC[111] NWs. Solid (dashed) lines indicate the relaxed (unrelaxed) nitrogen-doped NWs. The N occupation sites are indicated in Fig. 1. The zero energy is taken for the energetically more favorable configuration, namely, N_C at the NW surface in (a) and N_C occupying the inner sites of the NWs in (b) and (c).

electronic states are mostly composed by the B^c_{Si} $2p$ orbitals, where electronic contributions from the nearest-neighbor C and Si atoms are almost negligible. In contrast, for B^d_{Si} in SiC[111] NW, Fig. 5(c), the nearest-neighbor C and Si atoms contribute to the formation of $v1$ and $c1$. $v1$ lies at 0.45 eV above the VBM, and the $v1$-$c1$ energy split, 1.1 eV, is larger compared with the ones obtained for B^c_{Si} in SiC[100] NWs.

B. Nitrogen in SiC NWs

Figure 6 presents the relative formation energies (at the stoichiometric condition) of N_{Si} and N_C along the NW diameter. We find that the formation of N_{Si} in SiC NWs is quite unlikely. For Si/SiC[100] the formation energy of N_C changes only by 0.1 eV along the NW diameter [Fig. 6(a)], N^f_C being the energetically more favorable configuration. In contrast, the N_C segregation toward the C/SiC[100] NW sur-

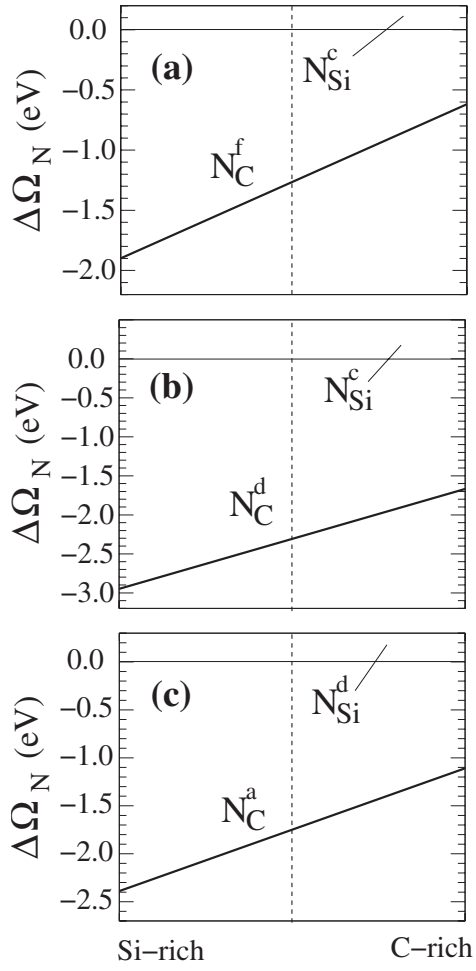

FIG. 7. Formation energies of substitutional N_C and N_{Si} ($\Delta\Omega_N$), as a function of the C chemical potential, in (a) Si/SiC[100], (b) C/SiC[100], and (c) SiC[111] NWs. At the C-rich (Si-rich) limit we have $\mu_C=\mu_C^{bulk}$ ($\mu_C=\mu_C^{bulk}-\Delta H^{3C\text{-}SiC}$). $\Delta\Omega_N$ is negative within the allowed energy range of the C chemical potential.

face is not expected to occur [Fig. 6(b)]. In this case, the formation energy increases as a function of the radial displacement of N_C atoms toward the surface, suggesting that the presence of energetically stable of C-H bonds somewhat suppresses the formation of N_C nearby the NW surface. Similar result has been obtained in SiC[111], Fig. 6(c), i.e., the formation energy of N_C increases near the NW surface. These results indicate that the N_C atoms do not segregate to the NW surface, N_C impurities at the inner sites of the hydrogenated C/SiC[100] and SiC[111] NWs being the energetically more favorable configuration. At the equilibrium geometry, the N_C is fourfold coordinated with the nearest-neighbor Si atoms, with N_C-Si bond lengths of 1.90–1.97 Å, i.e., slightly larger than the sum on the Si and N covalent radii. In 3C-SiC, we find N_C-Si bond distances of 1.96 Å.

Dashed lines in Fig. 6 indicate the formation energies N_{Si} and N_C calculated for the unrelaxed systems. We find that the relaxation energies of N_{Si} are larger at the surface sites, viz., 4.7, 3.8, and 4.5 eV for the Si/SiC[100], C/SiC[100], and SiC[111] NWs, respectively. However, those relaxation energies are not enough to promote the formation of N_{Si} at the NW surface. In contrast, for N_C the relaxation energies are practically the same along the NW diameter, being slightly larger at the NW surface. It is noticeable that even for the unrelaxed system, the formation of N_C at the core region of the C/SiC[100] and SiC[111] NWs represents the most likely configuration.

TABLE II. Calculated results of $\Delta\Omega$ (in eV) for N impurity in SiC.

	Core	Edge/subedge
Impurity	$\Delta\Omega^{(site)}$	$\Delta\Omega^{(site)}$
	Si/SiC[100] NW	
N_{Si}	$0.16^{(a)}$	$-4.40^{(c)}$
N_C	$-0.86^{(d)}$	$-0.90^{(f)}$
	C/SiC[100] NW	
N_{Si}	$-0.18^{(a)}$	$-3.63^{(c)}$
N_C	$-1.37^{(d)}$	$-0.63^{(f)}$
	SiC[111] NW	
N_{Si}	$-0.50^{(a)}$	$-4.02^{(d)}$
N_C	$-0.96^{(a)}$	$-0.74^{(d)}$

The relative formation energy ($\Delta\Omega_N$) as a function of the C chemical potential, depicted in Fig. 7, indicates that the formation of N_{Si} in SiC NWs ($\Delta\Omega_N>0$) is not expected even at the C-rich limit. However, due to the atomic relaxation nearby the NW surface, the formation energy differences between N_C and N_{Si} are smaller than the ones obtained for the SiC bulk phase. For instance, in Si/SiC[100] NW we find a formation energy difference of 0.6 eV ($\Delta\Omega_N=-0.6$ eV) between N_{Si}^c and N_C^f at the C-rich condition [Fig. 7(a)]. At the same C-rich condition, we find formation energy differences of 1.5 [Fig. 7(b)] and 1.1 eV [Fig. 7(c)], between N_C^a and N_{Si} occupying surface sites for C/SiC[100] and SiC[111] NWs, respectively. While in the 3C-SiC bulk, N_{Si} is energetically less stable than N_C by 5.4 eV at the C-rich limit.

For N impurities in SiC we examined their formation energies as a function of the host structural phase following the Eq. (3). Our results of $\Delta\Omega$ for N_{Si} and N_C are presented in Table II. In general, we obtained negative values of $\Delta\Omega$, thus, indicating that the formation of N-doped thin SiC NWs is easier compared with the same impurity in the 3C-SiC bulk phase. In particular for N_C impurities in thin and hydrogen-passivated C/SiC[100] and SiC[111] NWs, the energetic preference for the inner sites of SiC NWs suggests that the self-purification process does not take place in these N-doped hydrogen-passivated SiC NWs.

We next examined the electronic structure of the energetically more favorable configurations of N_C defects in SiC NWs. For Si/SiC[100], we find two spin unpaired electronic levels within the fundamental band gap. The highest occupied state is very localized and lies at ~1.2 eV above the VBM. Our calculated PDOS, Fig. 8(a), indicate that this state is mainly composed by the $2p$ and $3p$ orbitals of N_C and the

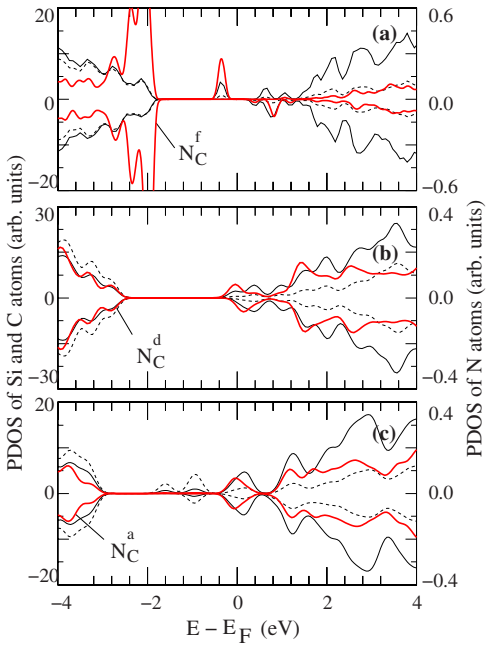

FIG. 8. (Color online) PDOS of (a) N_C-doped Si/SiC[100], (b) C/SiC[100], and (c) SiC[111] NWs. Solid thick (red) lines represent the PDOS of N atoms, and the solid (dashed) thin lines represent the PDOS of Si (c) atoms. We have considered a Gaussian (broadening) width of 0.2 eV, and the positive (negative) values of PDOS correspond to spin-up (spin-down) electronic densities.

nearest-neighbor (host) Si atoms, respectively. Meanwhile the lowest unoccupied state is less localized, and exhibits an energy dispersion of about 0.6 eV, being partially resonant within the conduction-band edge of the Si/SiC[100] NW. This lowest unoccupied state comes mostly from the antibonding $3p$ orbitals of the host Si atoms nearest neighbor to the N_C impurity. The electronic states induced by N_C at the inner sites of the C/SiC[100] NW are partially occupied, being resonant with the Si $3p$ antibonding states that compose the conduction-band edge [Fig. 8(b)]. These partially occupied states follow the energy dispersion of the conduction-band minimum, and the spin unpaired bands come from the $2p$ orbitals of N_C. In the SiC[111] NW, N_C also occupies the inner site of the NW; however, the electronic band structure presents a quite different picture with respect to the N_C impurity in the C/SiC[100] NW [see Fig. 8(c)]. There are no partially occupied states, and we find flat (occupied) energy bands within the fundamental band gap composed mostly by the $2p$ orbitals of host C atoms neighboring the N_C impurity. Meanwhile, electronic states of N_C are resonant with the Si $3p$ orbitals that compose the conduction-band edge. Based on those findings, for N_C lying at the inner sites of SiC NWs, we observe that the electronic properties of the N-doped thin SiC NWs depend on the NW growth direction.

IV. CONCLUSIONS

We have performed an *ab initio* total-energy investigation of B- and N-doped hydrogen-passivated SiC NWs. At the inner sites of the NWs, we find that the formation of B_C represents the most likely configuration. However, the B impurity atom segregates toward the surface, being B_{Si} at the NW surface the energetically more favorable configurations. Our total-energy results suggest that B impurities are expelled out from SiC NWs, independent of the NW growth direction. Thus, likewise B and P impurities in Si nanocrystals and Ge NWs, we can infer that the "self-purification" mechanism also takes place in B-doped SiC NWs. The electronic structure calculation of B_{Si} lying at the NW surface sites indicates the formation of localized spin unpaired impurity states within the fundamental band gap. For N impurity in SiC NWs we find a quite different scenario. The formation of N_{Si} is not expected to occur in SiC NWs. The formation energies of N_C at the core and surface sites of Si/SiC[100] NW are almost degenerated. Meanwhile in C/SiC[100] and SiC[111] NWs, the N_C impurity atom exhibits an energetic preference for the core sites of the NWs. Thus, different from B impurities in thin SiC NWs, we do not observe self-purification processes in N-doped SiC NWs. Further total-energy comparison indicates that the energy cost to the formation of N_C in SiC NWs is lower compared with its counterpart in the 3C-SiC bulk phase.

ACKNOWLEDGMENTS

The authors acknowledge financial support from the Brazilian agencies CNPq and FAPEMIG, and the computational support from CENAPAD/SP.

[1] S. C. Erwin, L. Zu, M. I. Haftel, A. L. Efros, T. A. Kennedy, and D. J. Norris, Nature (London) **436**, 91 (2005).
[2] G. M. Dalpian and J. R. Chelikowsky, Phys. Rev. Lett. **96**, 226802 (2006).
[3] M. H. Du, S. C. Erwin, A. L. Efros, and D. J. Norris, Phys. Rev. Lett. **100**, 179702 (2008).
[4] G. M. Dalpian and J. R. Chelikowsky, Phys. Rev. Lett. **100**, 179703 (2008).
[5] G. Cantele, E. Degoli, E. Luppi, R. Magri, D. Ninno, G. Iadonisi, and S. Ossicini, Phys. Rev. B **72**, 113303 (2005).
[6] T. L. Chan, M. L. Tiago, E. Kaxiras, and J. R. Chelikowsky, Nano Lett. **8**, 596 (2008).
[7] H. Peelaers, B. Partoens, and F. M. Peeters, Nano Lett. **6**, 2781 (2006).
[8] M. V. Fernández-Serra, Ch. Adessi, and X. Blase, Phys. Rev. Lett. **96**, 166805 (2006).
[9] H. Peelaers, B. Partoens, and F. Peeters, Appl. Phys. Lett. **90**, 263103 (2007).
[10] P. Mélinon, B. Masenelli, F. Tournus, and A. Perez, Nat. Mater. **6**, 479 (2007).
[11] G. Mpourmpakis, G. E. Froudakis, G. P. Lithoxoos, and J. Samios, Nano Lett. **6**, 1581 (2006).

[12] X.-H. Sun, C.-P. Li, W.-K. Wong, N.-B. Wong, C.-S. Lee, S.-T. Lee, and B.-K. Teo, J. Am. Chem. Soc. **124**, 14464 (2002).
[13] L. Z. Pei, Y. H. Tang, Y. W. Chen, C. Guo, X. X. Li, Y. Yuan, and Y. Zhang, J. Appl. Phys. **99**, 114306 (2006).
[14] L. Z. Pei, Y. H. Tang, Y. W. Chen, and C. Guo, J. Appl. Phys. **100**, 046105 (2006).
[15] R. Wu, J. Chen, G. Yang, L. Wu, S. Zhou, J. Wang, and Y. Pan, J. Cryst. Growth **310**, 3573 (2008).
[16] R. J. Baierle, P. Piquini, L. P. Neves, and R. H. Miwa, Phys. Rev. B **74**, 155425 (2006).
[17] R. J. Baierle and R. H. Miwa, Phys. Rev. B **76**, 205410 (2007).
[18] A. Gali, Phys. Rev. B **75**, 085416 (2007).
[19] A. V. Bolotnikov, P. G. Muzykov, and T. S. Sudarshan, Appl. Phys. Lett. **93**, 052101 (2008).
[20] R. Rurali, E. Hernandéz, P. Godignon, J. Rebollo, and P. Ordejón, Phys. Rev. B **69**, 125203 (2004).
[21] M. Bockstedte, A. Mattausch, and O. Pankratov, Phys. Rev. B **70**, 115203 (2004).
[22] K. Kojima, S. Kuroda, H. Okumura, and K. Arai, Appl. Phys. Lett. **88**, 021907 (2006).
[23] R. Rurali, P. Godignon, and J. Rebollo, Appl. Phys. Lett. **82**, 4298 (2003).
[24] J. M. Soler, E. Artacho, J. D. Gale, A. García, J. Junquera, P. Ordejón, and D. Sánchez-Portal, J. Phys.: Condens. Matter **14**, 2745 (2002).
[25] J. P. Perdew, K. Burke, and M. Ernzerhof, Phys. Rev. Lett. **77**, 3865 (1996).
[26] N. Troullier and J. L. Martins, Phys. Rev. B **43**, 1993 (1991).
[27] G. Theodorou, G. Tsegas, and E. Kaxiras, J. Appl. Phys. **85**, 2179 (1999).
[28] R. Rurali, Phys. Rev. B **71**, 205405 (2005).
[29] G.-X. Qian, R. M. Martin, and D. J. Chadi, Phys. Rev. B **38**, 7649 (1988).
[30] B. Aradi, P. Deák, N. T. Son, E. Jazén, W. J. Choyke, and R. P. Devaty, Appl. Phys. Lett. **79**, 2746 (2001).
[31] R. Rurali, P. Godignon, J. Rebollo, P. Ordejón, and E. Hernández, Appl. Phys. Lett. **81**, 2989 (2002).
[32] H. Woodbury and G. W. Ludwig, Phys. Rev. **124**, 1083 (1961).